International Journal of Multiphase Flow 35 (2009) 525–532

Contents lists available at ScienceDirect

International Journal of Multiphase Flow

journal homepage: www.elsevier.com/locate/ijmulflow

Nucleate boiling heat transfer in aqueous solutions with carbon nanotubes up to critical heat fluxes

Ki-Jung Park [a], Dongsoo Jung [a,*], Sang Eun Shim [b]

[a] Department of Mechanical Engineering, Inha University, Incheon 402-751, Republic of Korea
[b] Department of Chemical Engineering, Inha University, Incheon 402-751, Republic of Korea

ARTICLE INFO

Article history:
Received 27 October 2008
Received in revised form 16 February 2009
Accepted 17 February 2009
Available online 5 March 2009

Keywords:
Nucleate boiling
Nanofluids
Carbon nanotubes (CNTs)
Critical heat flux
Heat transfer coefficients

ABSTRACT

In this study, pool boiling heat transfer coefficients (HTCs) and critical heat fluxes (CHFs) are measured on a smooth square flat copper heater in a pool of pure water with and without carbon nanotubes (CNTs) dispersed at 60 °C. Tested aqueous nanofluids are prepared using multi-walled CNTs whose volume concentrations are 0.0001%, 0.001%, 0.01%, and 0.05%. For the dispersion of CNTs, polyvinyl pyrrolidone polymer is used in distilled water. Pool boiling HTCs are taken from 10 kW/m^2 to critical heat flux for all tested fluids. Test results show that the pool boiling HTCs of the aqueous solutions with CNTs are lower than those of pure water in the entire nucleate boiling regime. On the other hand, critical heat flux of the aqueous solution is enhanced greatly showing up to 200% increase at the CNT concentration of 0.001% as compared to that of pure water. This is related to the change in surface characteristics by the deposition of CNTs. This deposition makes a thin CNT layer on the surface and the active nucleation sites of the surface are decreased due to this layer. The thin CNT layer acts as the thermal resistance and also decreases the bubble generation rate resulting in a decrease in pool boiling HTCs. The same layer, however, decreases the contact angle on the test surface and extends the nucleate boiling regime to very high heat fluxes and reduces the formation of large vapor canopy at near CHF. Thus, a significant increase in CHF results in.

1. Introduction

At present, the whole world pays great attention to energy efficiency improvement and environmental protection due to global warming caused mainly by excessive use of fossil fuels. One of the fundamental ways of alleviating global warming is to increase the efficiency of the boilers in power plants, evaporators in refrigeration system, and various heat exchangers for commercial and domestic use. Especially, boiling heat transfer occurs in many of these heat exchangers and hence increasing boiling heat transfer coefficients (HTCs) is very important for global environmental protection. In fact, boiling heat transfer has been applied to many heat dissipation systems due to its high efficiency and much research has been done in the past for the examination of various aspects of boiling heat transfer.

Recently, nuclear power generation is discussed again in many countries as one of the alternative methods to solve energy crisis. For safe operation of nuclear power plants, ways of increasing critical heat flux (CHF) which is related to the loss of coolant accident are being investigated. In the event that local heat flux exceeds the CHF, there is an abrupt shift in boiling curve such that nucleate boiling ceases and transition boiling and ultimately film boiling occur and finally physical break down of the surface results in. This is due to the rapid increase in surface temperature caused by retarded heat transfer through the vapor blanket over the surface. Therefore, it is essential to maximize the CHF for the protection of nuclear power plants with maximum system performance.

For the past decade, as much research was carried out for the improvement of boiling HTCs and CHF, new methods employing nano particles have been proposed (Eastman et al., 1997; Lee et al., 1999; Keblinski et al., 2005; Wang and Mujumdar, 2007). For this purpose, some nano particles based upon mainly copper and aluminum which possess relatively high thermal conductivity have been developed. Nanofluids with such nano particles were shown to have high thermal conductivities (Eastman et al., 2001; Das et al., 2003a). Recently, some researchers performed pool boiling experiments with such nanofluids and observed an increase in CHF. You et al. (2003) dispersed Al_2O_3 particles in water and performed pool boiling experiments using a small square flat heater and observed more than 200% increase in CHF with the nanofluid as compared to that of pure water. They suggested that the concentration of nano particles, size and frequency of bubbles during nucleation have great influence on the increase in CHF. Bang and Chang (2005) also used the same Al_2O_3 particles in water and performed pool boiling experiments. They observed only 32% increase in CHF with the nanofluid and suggested that the nano particle deposition on the surface due to boiling caused a significant change in surface characteristics which in turn resulted in the increase in CHF.

* Corresponding author. Tel.: +82 32 860 7320; fax: +82 32 868 1716.
E-mail address: dsjung@inha.ac.kr (D. Jung).

0301-9322/$ - see front matter © 2009 Elsevier Ltd. All rights reserved.
doi:10.1016/j.ijmultiphaseflow.2009.02.015

Kim et al. (2007a) performed boiling experiments using nanofluids with alumina, zirconia, and silica particles and suggested more concrete reasons for the improvement of CHF with the nanofluids. They analyzed their experimental data with some theoretical equations to find reasons for the deposition of nano particles on the surface during boiling. They also tried to explain how the particle deposition decreased HTCs during nucleate boiling but increased the CHF. Consequently, they suggested that the particle deposition has influence on not only bubble formation as suggested by You et al. (2003) but also surface characteristics such as roughness and wettability.

Coursey and Kim (2008) performed pool boiling experiments using alumina dispersed water and ethanol with oxidized and non-oxidized surfaces in an attempt to explain the cause of the improvement in CHF. They observed that the oxidized surface showed 41% improvement in CHF as compared to the non-oxidized one. They also suggested that the contact angle plays an important role in increasing the CHF as proposed by Kim et al. (2007a).

Kim et al. (2007b) measured the CHF from a thin 0.2 mm diameter wire heater in aqueous solutions with TiO_2 and Al_2O_3 particles. They varied the particle volume concentration from 10^{-5}% to 10^{-1}% to examine the concentration effect on CHF. They observed 100% improvement in CHF of the nanofluids as compared to that of pure water. They attributed the improvement to the particle deposition and decrease in contact angle.

In this nucleate pool boiling study, carbon nanotubes (CNTs) are used instead of metal particles employed in other studies. The volume concentrations of the CNTs are changed to see if there is an optimum concentration for the maximum improvement of the CHF. CNTs have been known to have excellent mechanical, electrical, thermal, and optical properties and are regarded as one of the leading materials for information technology applications (Ajayan, 1999; Dresselhaus et al., 2001; Baughman et al., 2002). From the view point of thermal consideration, CNTs are very important since they are thermally super conductors whose thermal conductivity is 10 times that of gold (Ajayan, 1999; Dresselhaus et al., 2001). Due to their excellent thermal properties, CNTs are being considered as one of the means to improve boiling heat transfer.

Recently, Park and Jung (2007) measured pool boiling HTCs of water and R22 with and without CNTs from a long copper cylinder heater. They pre-treated the CNTs with acid for better dispersion and dispersed them into both fluids at the volume concentration of 1.0%. They measured pool boiling HTCs at heat fluxes below 100 kW/m^2, which is far below the CHF, and observed up to 30% increase in HTCs with CNTs. This is a significant finding since many researchers found that pool boiling HTCs are degraded with nano particles due to fouling (or scaling) effect (Das et al., 2003b,c; Bang and Chang, 2005; Kim et al., 2007a). Park and Jung (2007), however, did not observe fouling with acid treated CNTs and attributed the HTC improvement to the good thermal characteristics of CNTs. No research work, however, has been found in the literature on the effect of CNTs on pool boiling HTCs up to the CHF. The objectives of this study are to measure the nucleate pool boiling HTCs of water without and with CNTs at various volume concentrations up to the CHF and analyze the effect of CNTs on both nucleate boiling HTCs and CHF.

2. Experiments

2.1. Experimental apparatus

Fig. 1 shows the schematic of the experimental apparatus for nucleate boiling heat transfer tests with nanofluids. The apparatus is composed of mainly the boiling vessel and external condenser. The hermetically sealed boiling vessel was manufactured with a 170 mm long stainless steel pipe of 120 mm diameter and flanges at both ends. The vapor generated by the test heater in the vessel was condensed in the external condenser and the condensate was circulated to the bottom of boiling vessel via gravitation as shown in Fig. 1. The cooling water needed in the condenser was supplied by an independent precision chiller. For low vapor pressure fluids, sometimes it was difficult to lower the pool temperature to the desired value. Hence, a small copper tube coil was placed in the vessel through which cold water from the chiller was passed for adjusting the pool temperature. Also a cartridge heater was installed at the bottom of the vessel to adjust the temperature for initial heating. Since the main test heater used in this study was very small, heat loss to the surrounding may cause a significant uncertainty in the measurements. And hence, the boiling vessel, the external condenser, and all connecting pipes were thoroughly insulated with 20 mm thick insulation.

2.2. Heat transfer test section

In this study, a small flat plate heat transfer test section was manufactured to measure the nucleate boiling data up to the CHF. Fig. 2 shows the details of the test section. The test section was composed of a copper plate block and a heater supplying heat to the surface. The heater was a commercial square flat plate uniform heat generating resistor of 20 Ω (9.53 mm × 9.53 mm, CGI company, model: CCR-375-1) and could generate up to 3800 kW/m^2. A 4 mm thick square copper plate of the same size as the heater was machined since the heater itself could not be used as the heat transfer surface. After the selection of the heater and the copper plate, these two are bonded together using a silver solder.

As shown in Fig. 2, four holes (1.0 mm diameter, 5.0 mm length) were machined within the cooper plate, 2.0 mm away from the actual heat transfer surface with equal intervals and fine T-type (copper–constantan) thermocouples were inserted to these holes to measure directly the surface temperatures. And then, the holes were filled with a silver solder for uniform heating in the copper plate block.

In order for the heat from the heater to be transmitted upwardly to the copper plate block, a plastic insulation block (40.0 mm × 40.0 mm × 20.0 mm) was made with a very low thermal conductivity nylon. On the upper portion of the insulation block, a 5.0 mm deep rectangular section of 18.0 mm by 15.0 mm was machined to house the heater and copper plate block assembly. A 15.0 mm long hole of 13.0 mm diameter was machined in one side of the insulation block to accommodate a stainless steel pipe. Finally, the test heater assembly was put in the insulation block and electrical wires were carefully connected to the heater and the wires and four thermocouple wires were led out of the insulation block through the stainless steel pipe. Thus, these wires were not in direct contact with the working fluids. Finally, another epoxy that does not react with working fluids was applied to the gap between the heater assembly and stainless steel pipe and insulating block. The electrical wires were connected to a DC power supply (Agilent model 6030A, 200 V, 17 A).

2.3. Experimental details

Heat transfer performance of boiling surface tends to degrade over time due to a fouling effect (Webb, 1994). Therefore, it is important to maintain uniform surface condition for all tests to generate a reliable data set for various fluids. For this purpose, the surface of the heat transfer section was cleaned with #2000 emery paper and then cleansed with acetone whenever a fluid was changed. For fair comparison, HTCs were measured under the same steady-state condition at the same pool temperature of 60 °C for all fluids tested in this study, which was

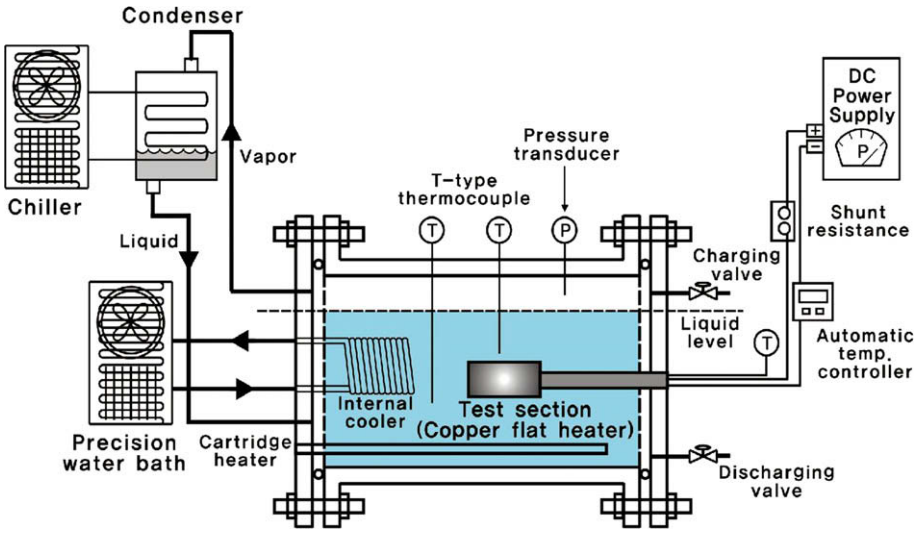

Fig. 1. Schematic of pool boiling test facility using a flat copper heater.

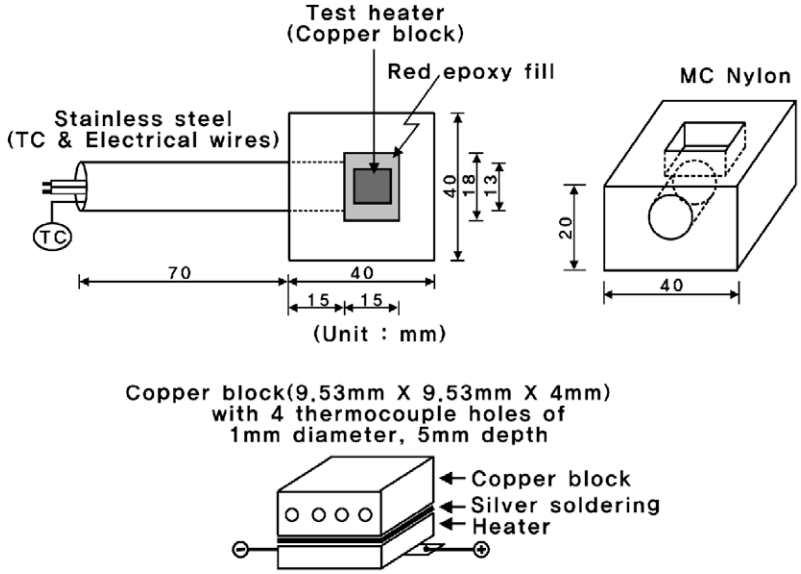

Fig. 2. Flat heater specifications.

accomplished mainly through the use of an external chiller shown in Fig. 1. For pure water, the pool was in vacuum at 19.9 kPa. The reason for keeping the pool temperature at 60 °C was due to the material limitation of the resistor heater. When the surface temperature exceeded 150 °C, the resistor heater broke down. To prevent this from happening, inevitably the measurements were taken at the pool temperature at 60 °C in vacuum under vacuum condition.

To measure the pool temperatures and pressure, two T-type thermocouples and a precision pressure transducer were mounted in the liquid and vapor spaces in the vessel, respectively, as shown in Fig. 1. All thermocouples used in this study were T-type and were calibrated against a temperature calibrator of 0.01 °C accuracy. On the other hand, the pressure transducer was calibrated against a pressure calibrator of 0.1 kPa accuracy. The power input to the heater was determined with the help of a shunt resistor (Yokogawa model 221509, 50 mV, 20 A).

The experimental procedure for a given fluid was as follows:

1. Nitrogen was charged to the test pool up to 2000 kPa with some halogenated refrigerants to check with a halogen detector if there was any leak.
2. A vacuum pump was turned on few hours to evacuate the system thoroughly and the fluid was charged to the system up to 50 mm higher than the top of the heat transfer block.
3. After 1 h, power to the test heater was initiated and the heat flux was increased to 10 kW/m^2 gradually. And data were taken under steady state at 60 °C from 10 kW/m^2 to the CHF. Heat flux was increased with an interval of 10 kW/m^2 up to 200 kW/m^2. Beyond 200 kW/m^2, heat flux was increased with an interval of 20–30 kW/m^2 up to the CHF.
4. Test fluid was changed and the same procedures of (1)–(3) were repeated after the surface was cleaned as described earlier.

During the tests for each fluid, much care was exercised as the heat flux approached the CHF. It was observed that as the heat flux approached the burn out point, the fluid motion was unstable and

all of a sudden the surface temperature sharply increased. To prevent the physical burn out from happening, the surface temperature was scanned continuously and the power supply to the heater was shut off as soon as the surface temperature exceeded 150 °C.

Since the vessel was thoroughly insulated, no subcooling was observed for pure water which was confirmed by measured water temperature and pressure inside the vessel. Since the amount of PVP was very small, it was assumed that the saturation temperature for water + PVP solutions would be unchanged. Thus, during the experiments, all data for water as well as water + PVP solutions were taken at the fixed pool temperature of 60 °C.

Since the distilled water containing very little amount of the dissolved gases was used throughout the tests, degassing was not done. During the tests, no significant boiling hysteresis at the inception occurred indicating that dissolved gas effect was indeed small.

2.4. Dispersion of CNTs

In this study, multi-walled CNTs synthesized by a thermal chemical vapor deposition method were used (approximately 97.5% pure, Iljin Nanotech, Korea). The CNTs have a diameter of 10–20 nm and length of 10–50 μm. In order to utilize CNTs in many applications, it is important to make CNTs soluble in liquids. To do so, CNTs are treated either chemically or physically. In chemical treatments, CNTs are covalently functionalized to have a hydroxyl or carboxyl group. Although the long term dispersion capability is superior, severe damages of the pristine structure and properties of CNTs are sometimes experienced during the chemical oxidation process using strong acids such as sulfuric and nitric acids. Furthermore, environmental pollution is inevitable in such treatments. On the other hand, physical treatment of CNTs in which CNTs are encapsulated by surfactants or dispersants does not have that kind of problem. Although the choice of solvent is limited, the physical method has significant merits; the process is quite simple and the structure and properties of CNTs are unchanged.

In this study, CNTs were dispersed in water by means of PVP (polyvinyl pyrrolidone; M_w = 40,000 g/mol, Wako Chemical) polymer. PVP is soluble in water and various polar solvents, and its wettability is excellent. PVP has been frequently used as a dispersant in coatings and nanofluids (O'Connell et al., 2001).

In this study, 300 wt% of PVP with respect to the amount CNT was incorporated in CNT dispersion in water. The dispersion state was monitored by measuring the transmittance of monochromatic light (λ = 880 nm) employing Turbiscan (Formulaction, France). Suspensions in flat-bottomed cylindrical glass tubes (70 mm height, 27.5 mm external diameter) were placed in the instrument and the transmission of light from suspensions was periodically measured along the height at room temperature. The transmission detector receives the light going out of the sample at 0° from the incident beam, while the backscattering detector receives the light scattered by the sample at 135° from the incident beam. The results from transmission are presented as the sedimentation profile, i.e., Δ transmission flux versus time. Fig. 3 shows the dispersion stability of CNT dispersed aqueous solutions in which the variations of transmittance of light with time are compared for CNTs/water and CNTs/PVP/water dispersions. When CNTs are directly dispersed in water only by sonication for 10 min, the transmittance steadily increases with time, showing the sedimentation behavior of CNTs. On the other hand, the transmittance remains unchanged for the PVP-incorporated CNT dispersion, indicating excellent dispersion stability over 24 h. After 15 days, most of CNTs are sedimented for CNTs/water dispersion but excellent dispersion state are well maintained for CNTs/PVP/water dispersion.

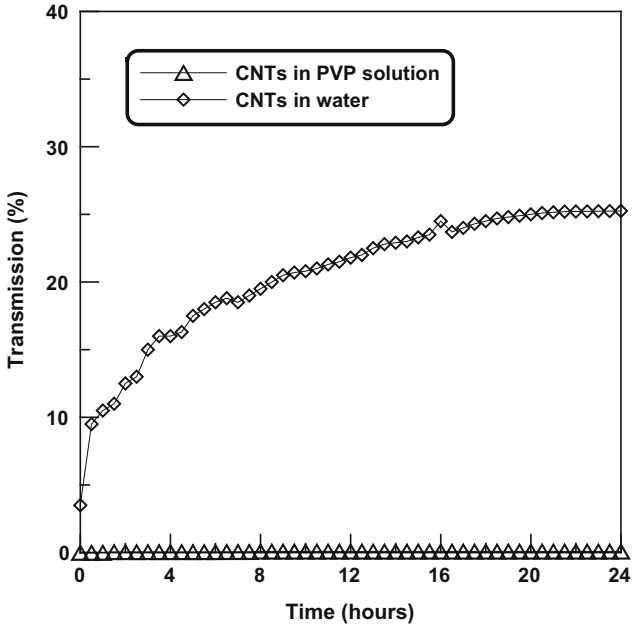

Fig. 3. Light transmission test results for the dispersion of CNTs in water and PVP solution.

2.5. Data reduction

In this study, heat transfer coefficient (HTC) was determined by the following equation:

$$h = \frac{Q/A}{(T_{wall} - T_{sat})} \tag{1}$$

where h, Q, A, T_{wall}, T_{sat} are the heat transfer coefficient (W/m^2 K), power input to the heater (W), heat transfer area (m^2), and average surface and liquid temperatures (°C), respectively.

The heat flux was calculated by the power input to the resistor heater and surface area of the heater. In this calculation, the heat loss to the bottom and all sides was assumed to be negligible since they were thoroughly insulated by low conductivity epoxy and plastic. Of course, there would be heat loss but that would be very small as compared to the heat going upward through copper surface with boiling heat transfer.

As mentioned earlier, the actual surface of the boiling block is 2.0 mm away from the thermocouple holes and hence the surface temperature, T_{wall}, in Eq. (1), needs to be modified from the measured average surface temperature, T_{th}, by applying an 1-D heat conduction equation as follows:

$$T_{wall} = T_{th} - \frac{Q}{A}\left[\frac{L}{k}\right] \tag{2}$$

where T_{th}, L, k are the measured average wall temperature by thermocouples (°C), distance from the hole to the surface (m), and thermal conductivity of the test section (W/m K), respectively.

Since the heat transfer block was made of copper, the temperature compensation term in Eq. (2), ($T_{th} - T_{wall}$), was small at low heat fluxes. But at high heat fluxes beyond 200 kW/m^2, the term was greater than 1 °C and hence could not be neglected in HTC determination.

For all fluids tested, measurements were taken at least three times under the same condition to check the repeatability. For each measurement, the surface was polished and thoroughly cleansed before testing and the repeatability was good showing less than 5% deviation.

The measurement uncertainties were estimated by the method suggested by Kline and McClintock (1953) and turned out to be less than 7.3% at all heat fluxes. In pool boiling heat transfer, the repeatability is very important and hence many measurements were taken repeatedly with an interval of 1 week to 1 month for many fluids to check the repeatability. Overall the repeatability was always within 5% which was within the measurement uncertainties.

3. Results and discussion

In this study, pool boiling HTCs are measured from a square flat heater, immersed in water at 60 °C, up to the CHF with and without CNTs dispersed at various concentrations to examine the effect of CNTs on boiling HTCs and CHF.

3.1. Confirmation of test result with well-known correlations

Before discussing the results, the measured data with pure water are compared with other researchers' data and theoretical correlations to check the reliability of the test apparatus and method. Fig. 4 shows the comparison. Even though there is a deviation in measured HTCs at heat fluxes above 200 kW/m^2, the present HTCs and You et al.'s (2003) agree within 10% in the entire heat flux range.

In nucleate pool boiling heat transfer with water, Rohsenow's (1952) correlations have been used popularly. Eq. (3) shows Rohsenow's correlation:

$$h = \frac{1}{C_{sf}}\left[\frac{C_{pf}q''}{h_{fg}}\right]\left[\frac{q''}{\mu_f h_{fg}}\left(\frac{\sigma}{g(\rho_f-\rho_g)}\right)^{1/2}\right]^{-1/3}\mathrm{Pr}^{-n} \quad (3)$$

where C_{sf}, C_{pf}, h_{fg}, q'', μ_f, σ, g, ρ_f, ρ_g, Pr are the surface-liquid coefficients, specific heat (kJ/kg K), heat of vaporization (kJ/kg), heat flux (kW/m^2), viscosity (μPa s), surface tension of the saturated liquid (N/m), gravitational acceleration (m/s^2), densities of saturated liquid and vapor (kg/m^3), and Prandtl number, respectively.

Rohsenow presented C_{sf} and n in Eq. (3) for various surface and fluid combination. For the present case of copper surface and water, the suggested values of C_{sf} and n are 0.0086 and 1.0. The predicted HTCs with those constants agreed with the present data within 5% deviation.

For the prediction of CHF of pure fluids, Zuber's (1959) correlation, Eq. (4), has been used widely for the past years.

$$q''_{CHF} = \frac{\pi}{24}h_{fg}\rho_g^{1/2}\left[g\sigma(\rho_f-\rho_g)\right]^{1/4} \quad (4)$$

The predicted CHF by Zuber's correlation is 560.5 kW/m^2 which is in excellent agreement with the present data of 560 kW/m^2. On the other hand, You et al.'s (2003) measured CHF was 540 kW/m^2 which is also good agreement with the present data. From this comparison, the reliability of the test apparatus and method was confirmed.

3.2. Pool boiling HTCs of nanofluids with CNTs

Fig. 5 shows the pool boiling HTCs obtained from a flat square heater as a function of heat flux for various nanofluids of differing CNT concentrations. Pool boiling HTCs of aqueous solutions with CNTs increased as the heat flux increased, which is a typical trend in pool boiling of pure fluids. At heat fluxes higher than the CHF of pure water (560 kW/m^2), no comparison can be made against pure water data. As for the nanofluids, as the CNT concentration increased, nucleate boiling HTCs decreased clearly. At heat fluxes lower than the CHF of pure water (560 kW/m^2), the trend was very similar. As the CNT concentration increased, HTCs of the aqueous solutions with CNTs decreased as compared to those of pure water. When CNTs are dispersed in water, CNTs are deposited on the heater surface during the bubble formation and form a thin layer which acts to reduce active nucleation sites. The reduction in active sites directly impedes the bubble formation and consequently results in reduction in HTCs.

Kim et al. (2007b) reported that this kind of nano particle deposited film causes an additional thermal resistance which in turn contributes to the reduction in boiling HTCs. The increase in thermal resistance, however, can not be quantified. The reduction of nucleate boiling HTCs due to fouling effect by the nano film was also seen in Bang and Chang's (2005) results.

Since most of the heat exchangers are operated under the heat flux lower than 200 kW/m^2, it is important to observe changes in

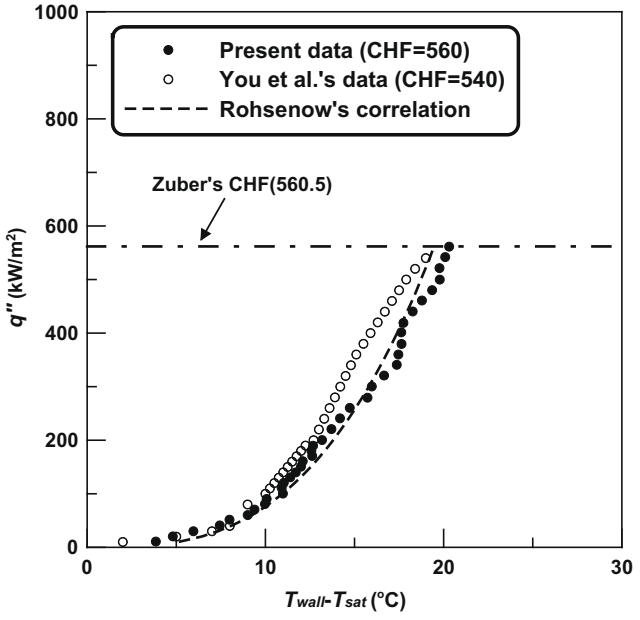

Fig. 4. Comparison of pure water data with You et al.'s data and some well-known correlations.

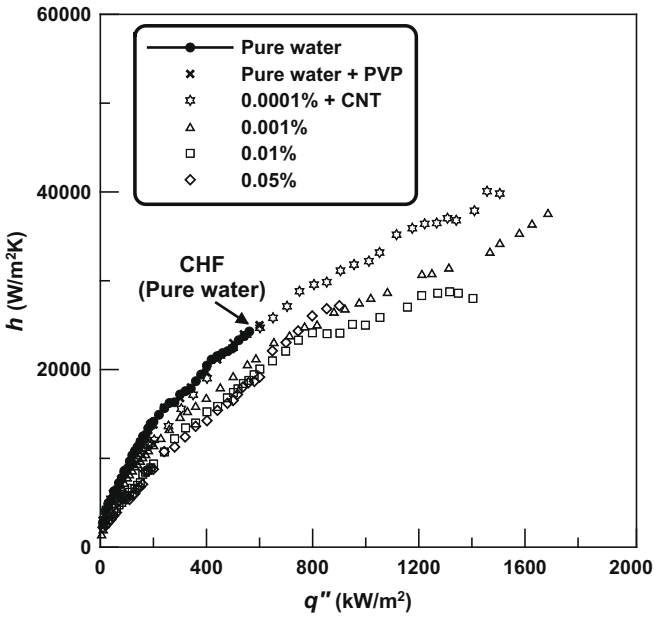

Fig. 5. Heat transfer coefficients of CNT nanofluids up to critical heat fluxes.

HTCs due to the addition of CNTs at low heat fluxes. Fig. 6 shows the pool boiling HTCs in detail at heat fluxes lower than 200 kW/m^2. Again, pool boiling HTCs decreased as the CNT concentration increased as seen at high heat fluxes. At the concentrations of 0.0001%, 0.001%, 0.01%, and 0.05% CNT, the average decrease in boiling HTCs of the aqueous solutions in the heat flux of 10–200 kW/m^2 were 7.4%, 22.3%, 34.0%, and 38.2%, respectively, as compared to those of pure water.

These results are in contradiction with Park and Jung's (2007) results obtained with the same multi-walled CNTs dispersed in water. In fact, they observed an increase in HTCs as CNTs were dispersed in water. The discrepancy seems to be caused by the difference in dispersion methods. In the present study, CNTs were dispersed physically using polymer dispersant of PVP. But in Park and Jung's (2007) study, CNTs were treated chemically using acid without employing polymers. Thus, Park and Jung (2007) did not observe nano particle deposition or fouling effect and saw an increase in HTCs of up to 30% at heat flux lower than 100 kW/m^2. In the present study, one can easily see the CNT deposited black surface film after experiments. Judging from these results, it is thought that the PVP polymer used in this study caused CNTs to be deposited on the surface during boiling and thus pool boiling HTCs decreased even at low heat fluxes. A further study of pool boiling HTCs measurements using acid treated CNTs up to the CHF is needed to verify this finding.

Since a dispersant was used for the dispersion of CNTs in water, it is important to examine the effect of the dispersant alone on boiling HTCs. As seen in Figs. 5 and 6, HTCs of water with the PVP dispersant were very similar to those with pure water. From this, it can be concluded that the PVP dispersant alone does not play any significant role in HTCs in the entire heat flux range. But the same dispersant causes CNT deposition on the surface in the aqueous solutions with CNTs and this consequently results in the reduction of boiling HTCs in the entire heat flux range.

3.3. Critical heat fluxes of nanofluids with CNTs

Fig. 7 shows the pool boiling heat transfer test results up to the CHF from a flat heater for various CNT concentrations and Table 1 lists CHFs for six fluids including pure water. First of all, it can be seen that CHFs of all aqueous solutions increased at all CNT concentrations as compared to that of pure water. The aqueous solution at the CNT concentration of 0.0001% showed 168% improvement in CHF as compared to that of pure water. On the other hand, the aqueous solutions at the CNT concentrations of 0.001% and 0.01% showed 200% and 150% improvement, respectively, as compared to that of pure water. As the CNT concentration increased from 0.0001% to 0.001%, the CHF increased as well. But the CHF of the aqueous solution at the CNT concentration of 0.01% decreased by 16.6% as compared to that of the solution at the CNT concentration of 0.001%. Further measurements were taken at the CNT concentration of 0.05% to see the effect of CNT concentration on CHF. As listed in Table 1, the CHF at the CNT concentration of 0.05% was 900 kW/m^2, which was 60.7% higher than that of pure water but was much lower than that at the CNT concentration of 0.01%. From these results, it can be concluded that the maximum CHF occurs at the CNT concentration of 0.001% for the aqueous solution with the multi-walled CNTs with the PVP polymer dispersant.

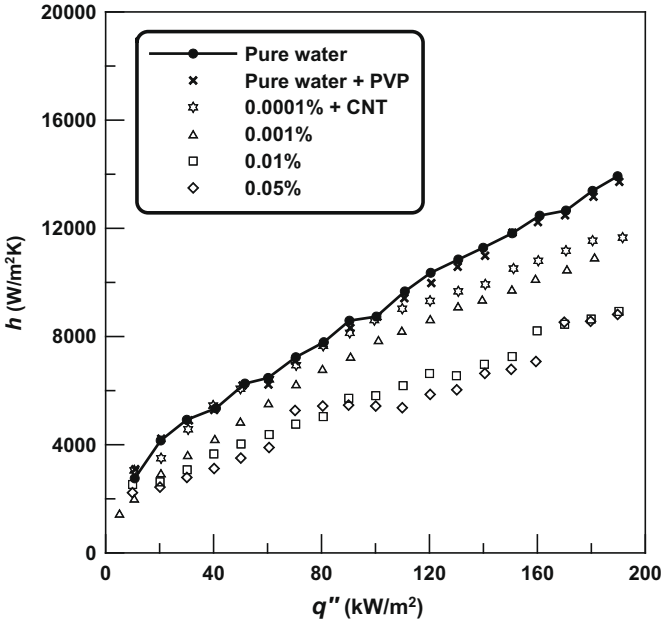

Fig. 6. Heat transfer coefficients of CNT nanofluids up to 200 kW/m^2.

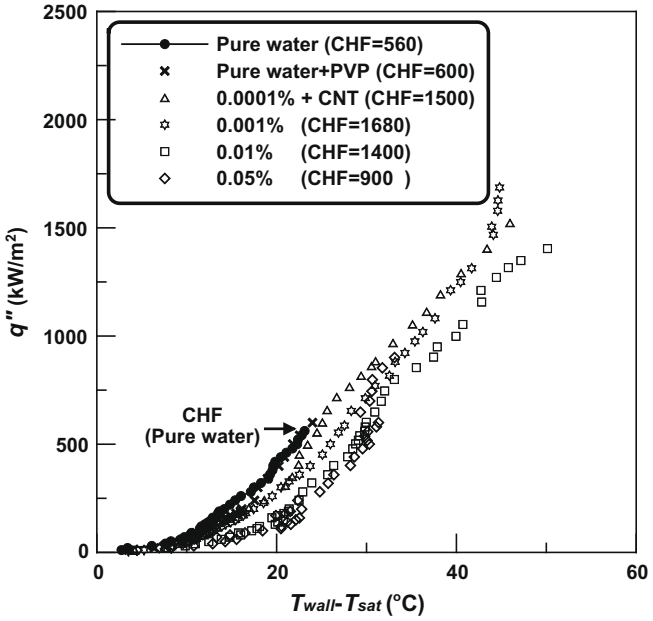

Fig. 7. Pool boiling data up to critical heat fluxes for all tested fluid.

Kim et al. (2007b) measured CHFs from a wire heater using TiO_2 and Al_2O_3 particles dispersed in water and reported that nano particles are deposited on the surface when nucleate boiling occurs in nanofluids and thus generated surface modifications result in an increase in CHF. Since no tests were carried out with aqueous solutions with CNTs, similar tests were carried out in this study using a 0.25 mm diameter, 50 mm long titanium wire heater at atmospheric pressure. Since the experimental apparatus was similar to that used by Kim et al. (2007b), details will not be repeated here and an interested reader is referred to their work. With the wire heater, the deposition of CNTs on the entire wire can be easily examined by a scanning electron microscope (SEM) since the diameter is very small and the CHF can be measured by increasing power until the wire collapses. The geometry of the wire heater, however, is not flat and hence the data generated with the wire heater can not be directly applied to the most of the flat surfaces (Kim et al., 2007a). Accordingly, measurements were carried out to obtain more or less qualitative data.

The same aqueous solutions with CNTs at the same concentrations were used in the titanium wire heater experiments and after experiments were done, the broken wires were placed on SEM for

Table 1
Critical heat fluxes of tested fluids.

Fluids	CHF (kW/m^2)	Increase as compared to pure water (%)
Pure water	560	
Pure water + PVP	600	7.1
+ PVP/CNT 0.0001%	1500	167.9
+ PVP/CNT 0.001%	1680	200.0
+ PVP/CNT 0.01%	1400	150.0
+ PVP/CNT 0.05%	900	60.7

taking images of the surfaces. Fig. 8 shows the CHFs as a function of the CNT concentration for both flat and wire heaters. As with the flat heater, the CHF with a wire heater increased as the CNT concentration increased. But beyond certain concentration, the CHF does not increase noticeably. For the wire heater, the CHFs also increased as compared to that of pure water at all CNT concentrations. At the CNT concentration of 0.0001%, the CHF was 40% higher than that of pure water while at the CNT concentrations of 0.001% and 0.01%, the CHFs were 140% higher than that of pure water.

Fig. 9 shows the magnified images of the surfaces of the titanium wire, which were taken by SEM after CHFs, were experienced. As seen in Fig. 9, the titanium wire had longitudinal grooves before experiments. There was little change in the surface after performing pool boiling tests up to the CHF in pure water. As the experiments are performed in the aqueous solutions with CNTs, however, the amount of CNT deposition on the surface increased as the CNT concentration increased as shown in Fig. 9. At the CNT concentrations of 0.0001% and 0.001%, CNTs were deposited uniformly on the surface. But at the CNT concentration of 0.01%, CNT deposition was excessive and CNTs were conglomerated on the surface. From these images, it can be concluded that there is an optimum CNT concentration and at concentrations beyond this optimum value, nano particle deposition is too much to increase the CHF. This result is in agreement with You et al.'s (2003) result that the CHF improvement is not seen when the amount of nano particles exceeds a certain value.

Kim et al. (2007b) showed that nano particle deposition is not caused by single phase turbulent flow or gravitational force but

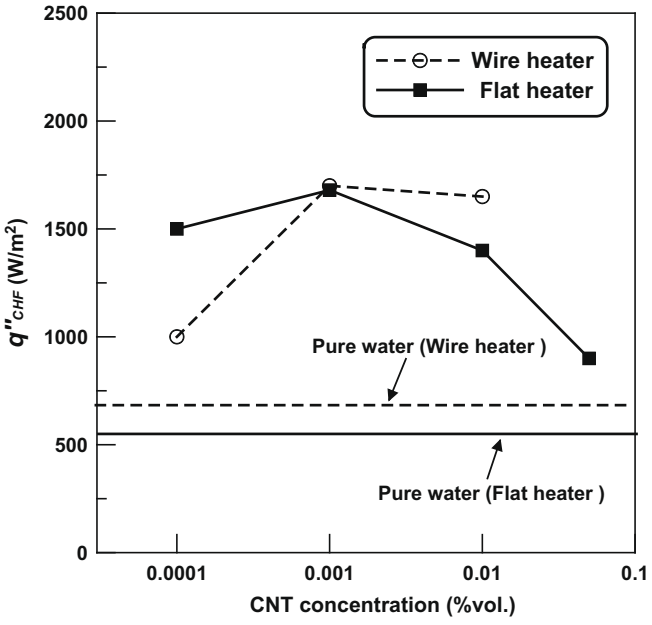

Fig. 8. Critical heat fluxes obtained from wire and flat heaters as a function of CNT concentration.

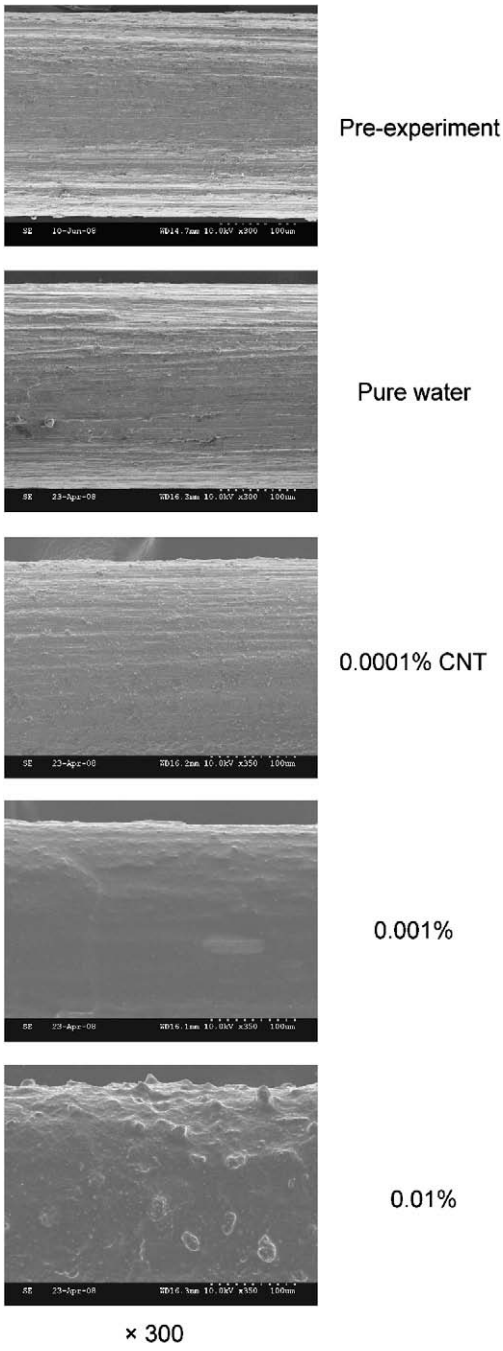

Fig. 9. SEM images of deposition of CNTs on heat transfer wire for various concentrations of CNTs (×300).

by the bubble formation and departure during active nucleate boiling. The present result indicates that their observation is also true of the aqueous solutions with CNTs.

Kim et al. (2007a) suggested that the decrease in contact angle due to nano particle deposition is one of the reasons for the improvement in CHF. Fukada et al. (2004) performed experiments using a wire heater and deposited some materials with higher wettability and observed that the CHF was increased by 167%. From these tests, Fukada et al. (2004) proved that the decrease in contact angle indeed has a significant impact on the improvement of CHF. Kandlikar (2001) confirmed that there is a strong relationship between the CHF and contact angle and suggested a CHF predicting correlation which utilizes a contact angle, Eq. (5).

$$\frac{q''_{CHF}}{h_{fg}\rho_g^{1/2}\left[g\sigma(\rho_f-\rho_g)\right]^{1/4}} = \left(\frac{1+\cos\beta}{16}\right)\left(\frac{2}{\pi}+\frac{\pi}{4}(1+\cos\beta)\right)^{1/2} \quad (5)$$

where β is the contact angle.

In fact, Eq. (5) is a modified version of Zuber's correlation, Eq. (4). While the right hand side of Kandlikar's correlation is a function of the contact angle, Zuber's correlation sets the right hand side as a constant value of 0.131.

To test Kandlikar's correlation, contact angles are measured for pure water and aqueous solutions with CNTs at the CNT concentration of 0.001% on copper surface after pool boiling experiments. Thus the copper surface was coated with CNTs for the aqueous solution with CNTs. The contact angles for these fluids on tested surfaces are measured to be $71 \pm 2^\circ$ and $30 \pm 1^\circ$, respectively. In this study, only the effect of contact angle is examined under the assumption that all physical properties in the left hand side of Eq. (5) remain the same. When the measured contact angles are put into the right hand side of Eq. (5), the CHF of the aqueous solution at the CNT concentration of 0.001% is predicted to be 60% higher than that of pure water. The actual test results, however, show that the CHF of the aqueous solution with CNTs at the CNT concentration of 0.001% is 200% higher than that of pure water. Hence, one can see that the decrease in contact angle alone does not explain the unusually high increase in measured CHF with the aqueous solution with CNTs. It is quite likely that the decrease in active nucleation sites due to the nano particle deposition extends the nucleate boiling regime to high heat fluxes and hence the CHF increases even though the nucleate boiling HTCs decrease.

Finally, the effect of the PVP polymer on the CHF was investigated. For this, some experiments were carried out with the PVP polymer added water. As seen in Fig. 7, there is little change in CHF when the PVP polymer alone is added to pure water. The contact angle was measured also for water solution with PVP but was not changed at all from that of pure water. From this, it can be concluded that the PVP dispersant used for the dispersion of CNTs does not play any role in CHF and the improvement in CHF with aqueous solutions with CNTs is caused solely by CNTs.

4. Conclusions

In this study, pool boiling HTCs were measured from a square flat heater (9.53 mm × 9.53 mm), immersed in water at 60 °C, up to CHFs with and without CNTs dispersed at various volume concentrations to examine the effect of CNTs on nucleate boiling HTCs and CHF. The CNT volume concentrations tested were 0.0001%, 0.001%, 0.01%, and 0.05%. For the dispersion of CNTs in water, a PVP polymer dispersant was used. From the test results, the following conclusions were drawn:

(1) When CNTs are dispersed in water, CHFs of all aqueous solutions increased at all CNT concentrations as compared to that of pure water. For multi-walled CNTs with the PVP polymer dispersant used in this study, the optimum CNT concentration was 0.001% and the CHF at that concentration increased 200% as compared to that of pure water.
(2) When CNTs were dispersed in water, they were deposited on the surface during bubble formation and departure. The surface images taken by SEM after CHF experiments showed that as the CNT concentration increased, the CNT deposition on the surface also increased. But beyond the optimum CNT concentration of 0.001%, CNTs were conglomerated and the CHF began to decrease.
(3) When CNTs were dispersed in water, the nucleate boiling HTCs decreased as the CNT concentration increased. As the nucleate boiling progressed, CNTs were deposited to form a thin film on the surface and the contact angle decreased. Because of this deposition, the probability of forming large vapor blanket by bubbles at high heat flux decreased and consequently, the CHF increased. The surface deposition, however, acts as a thermal resistance to reduce the bubble generation and in turn the reduction in boiling HTCs occurs in the entire nucleate boiling range.

Acknowledgement

This work was supported by the Korea Science and Engineering Foundation (KOSEF) grant funded by the Korean government (MOST) (No. R01-2007-000-20055-0).

References

Ajayan, P.M., 1999. Nanotubes from carbon. Chem. Rev. 99, 1787–1799.
Bang, I.C., Chang, S.H., 2005. Boiling heat transfer performance and phenomena of Al_2O_3–water nanofluids from a plain surface in a pool. Int. J. Heat Mass Transfer 48, 2407–2419.
Baughman, R.H., Zakhidov, A.A., de Heer, W.A., 2002. Carbon nanotubes – the route toward applications. Science 297, 787.
Coursey, J.S., Kim, J., 2008. Nanofluid boiling: the effect of surface wettability. Int. J. Heat Fluid Flow 29, 1577–1585.
Das, S.K., Putra, N., Thiesem, P., Roetzel, W., 2003a. Temperature dependence of thermal conductivity enhancement for nanofluids. ASME J. Heat Transfer 125, 567–574.
Das, S.K., Putra, N., Roetzel, W., 2003b. Pool boiling characteristics of nanofluids. Int. J. Heat Mass Transfer 46, 851–862.
Das, S.K., Putra, N., Roetzel, W., 2003c. Pool boiling of nanofluids on horizontal narrow tubes. Int. J. Multiphase Flow 29, 1237–1247.
Dresselhaus, M.S., Dresselhaus, G., Avouris, P. (Eds.), 2001. Carbon Nanotubes: Synthesis, Structure. Properties and Applications. Springer, New York. vol. 80.
Eastman, J.A., Choi, S.U.S., Li, S., Thompson, L.J., Lee, S., 1997. Enhanced thermal conductivity through the development of nano-fluids. In: Proceedings of the Symposium on Nanophase and Nanocomposite Materials II, Materials Research Society, Boston, vol. 457, pp. 3–11.
Eastman, J.A., Choi, S.U.S., Yu, W., 2001. Anomalously increased effective thermal conductivity of ethylene glycol-based nanofluids containing copper nanoparticles. Appl. Phys. Lett. 78, 718–720.
Fukada, Y., Haze, I., Osakabe, M., 2004. The effect of fouling on nucleate pool boiling of small wires. Heat Transfer-Asian Res. 33, 316–329.
Kandlikar, S.G., 2001. A theoretical model to predict pool boiling CHF incorporating effects of contact angle and orientation. ASME J. Heat Transfer 123, 1071–1079.
Keblinski, P., Eastman, J.A., Cahill, D.G., 2005. Nanofluids for thermal transport. Mater. Today 8, 36–44.
Kim, S.J., Bang, I.C., Buongiorno, J., Hu, L.W., 2007a. Surface wettability change during pool boiling of nanofluids and its effect on critical heat flux. Int. J. Heat Mass Transfer 50, 4105–4116.
Kim, H.D., Kim, J., Kim, M.H., 2007b. Experimental studies on CHF characteristics of nano-fluids at pool boiling. Int. J. Multiphase Flow 33, 691–706.
Kline, S.J., McClintock, F.A., 1953. Describing uncertainties in single-sample experiments. Mech. Eng. 75, 3–9.
Lee, S., Choi, U.S., Li, S., Eastman, J.A., 1999. Measuring thermal conductivity of fluids containing oxide nanoparticles. ASME J. Heat Transfer 121, 280–289.
O'Connell, M.J., Boul, P., Ericson, L.M., Huffman, C., Wang, Y., Haroz, E., Kuper, C., Tour, J., Ausman, K.D., Smalley, R.E., 2001. Reversible water-solubilization of single-walled carbon nanotubes by polymer wrapping. Chem. Phys. Lett. 342, 265–271.
Park, K.J., Jung, D., 2007. Enhancement of nucleate boiling heat transfer using carbon nanotubes. Int. J. Heat Mass Transfer 50, 4499–4502.
Rohsenow, W.M., 1952. A method of correlation heat-transfer data for surface boiling of liquids. ASME Trans. 74, 969–976.
Wang, X.-Q., Mujumdar, A.S., 2007. Heat transfer characteristics of nanofluids: a review. Int. J. Therm. Sci. 46, 1–19.
Webb, R.L., 1994. Principles of Enhanced Heat Transfer. Wiley, New York.
You, S.M., Kim, J.H., Kim, K.H., 2003. Effect of nanoparticles on critical heat flux of water in pool boiling heat transfer. Appl. Phys. Lett. 83, 3374–3376.
Zuber, N., 1959. Hydrodynamic aspects of boiling heat transfer, AEC Report No. AECU-4439, Physics and Mathematics.